

**Short Title: Comparison of *Withania* plastid genomes**

**Comparative Plastomics of Ashwagandha (*Withania*, Solanaceae) and Identification of Mutational Hotspots for Barcoding Medicinal Plants**

Furrukh Mehmood<sup>1,2</sup>, Abdullah<sup>1</sup>, Zartasha Ubaid<sup>1</sup>, Yiming Bao<sup>3</sup>, Peter Poczai<sup>2\*</sup>, Bushra Mirza<sup>\*1,4</sup>

<sup>1</sup>Department of Biochemistry, Quaid-i-Azam University, Islamabad, Pakistan

<sup>2</sup>Finnish Museum of Natural History, University of Helsinki, Helsinki, Finland

<sup>3</sup>National Genomics Data Center, Beijing Institute of Genomics, Chinese Academy of Sciences, Beijing, China

<sup>4</sup>Lahore College for Women University, Pakistan

\*Corresponding authors: **Bushra Mirza (bushramirza@qau.edu.pk)**

**Peter Poczai (peter.poczai@helsinki.fi)**

## Abstract

Within the family Solanaceae, *Withania* is a small genus belonging to the Solanoideae subfamily. Here, we report the *de novo* assembled, complete, plastomed genome sequences of *W. coagulans*, *W. adpressa*, and *W. riebeckii*. The length of these genomes ranged from 154,198 base pairs (bp) to 154,361 bp and contained a pair of inverted repeats (IRa and IRb) of 25,027--25,071 bp that were separated by a large single-copy (LSC) region of 85,675--85,760 bp and a small single-copy (SSC) region of 18,457--18,469 bp. We analyzed the structural organization, gene content and order, guanine-cytosine content, codon usage, RNA-editing sites, microsatellites, oligonucleotide and tandem repeats, and substitutions of *Withania* plastid genomes, which revealed close resemblance among the species. Both the substitution and insertion and deletion analyses confirmed that the IR region was significantly conserved compared with the LSC and SSC regions. Further comparative analysis among the *Withania* species highlighted 30 divergent hotspots that could potentially be used for molecular marker development, phylogenetic analysis, and species identification.

## Key words:

Ashwagandha, Chloroplast genome, InDels, Medicinal plants, Mutational hotspots, Phylogenomics, Solanaceae, Substitutions, *Withania*

## INTRODUCTION

The plant family Solanaceae consists of ~ 93 genera and ~ 2700 species [1,2]. This megadiverse family is comprised of species ranging from herbaceous annuals to perennial trees, with a natural distribution ranging from deserts to rainforests [3]. The genus *Withania* Pauq., belonging to the subfamily Solanoideae, contains ~10--20 species [1]. Among the worldwide list of *Withania* species, ashwagandha or winter cherry (*W. somnifera* (L.) Dunal) and paneer booti or ashutosh booti (*W. coagulans* (Stocks) Dunal) are considered highly important, due to their therapeutic potentials. These species play an important role in the indigenous medicine of Southeast Asia [4]. *Withania somnifera* has been used for over 3,000 years in the Ayurvedic medicine system [5]. Many studies of *Withania* have described the pharmacological properties of these species [6–9].

The ubiquity of such herbal products has expanded globally during recent decades. The worldwide market for medicinal plants is anticipated to reach 5 trillion USD by 2050, with Europe driving the market [10]. Medicinal plants are outstanding sources of innovative drug development, but assessing their pharmacological properties and effectiveness requires thorough approaches. Irregularities are calling attention to the quality of traded mass-produced herbal products manufactured from ashwagandha (*Withania* species), with direct impact on their efficacy and safety [11]. The quality of these manufactured herbal products is highly variable globally, and consistent analytical approaches are required to identify and monitor their quality along the value chain. DNA barcoding has become a major focus in the herbal medicine industry, because it can be used to consistently apply quality control over the manufactured products and to identify medicinal materials to protect consumers from being duped by dishonest suppliers. In addition, DNA barcoding can serve as a forensic tool to aid in detecting toxic herbal materials in life-threatening situations, prevent poisoning, and improve control procedures of herbal drug substances [12].

The structure and composition of the chloroplast (cp) genome can be utilized to generate molecular markers that can be used in DNA barcoding [13]. Cps are important and universal organelles that play a vital role in photosynthesis and are also associated with biochemical pathways, such as the biosynthesis of fatty acids, amino acids, vitamins, and pigments [14]. Among the many plant species, plastid genomes are about 75-250 kilobases (kb) in size [15] and contain ~120 genes, which include protein-encoding genes, ribosomal RNA (rRNA), and transfer RNA (tRNA) [16]. Angiosperm plastomes occur in circular and linear forms [17], and the percentage of each varies within plant cells [17]. Circular-formed plastomes are typically quadripartite in structure, with a pair of inverted repeats (IRa and IRb) regions, segregated by a large single-copy (LSC) and a small single-copy (SSC) region [15,18,19]. Numerous mutational events occur in plastid genomes: variations in tandem repeat numbers, insertions and deletions (InDels), point mutations, inversions and translocations [19–21]. Plastomes have been termed as ‘superbarcodes’, due to their comparatively conserved organization, gene content, slow rate of nucleotide substitution in protein-encoding genes, and uniparental inheritance, which make them excellent sources of phylogenetic reconstruction and species identification at diverse taxonomic levels [22–25]. Plastome-sequencing data can also be useful for agricultural trait improvement [26],

transplastomics [27,28], population genetics [29], and conservation of species facing extinction [30].

Here, we aimed to assemble and compare the plastid genome sequences of *W. coagulans*, *W. adpressa* Coss., and *W. riebeckii* Schweinf. ex Balf.f. to reveal differences in their organization and characteristics in repeats, insertion-deletions, and single-nucleotide polymorphisms (SNPs), as well as to identify mutational hotspots for DNA barcoding. We also inferred the phylogeny of *Withania*, based on our sampling, to determine the utility of the polymorphic loci detected in species identification.

## MATERIALS AND METHODS

### Genome assembly and annotation

Fresh lush green leaves of *W. coagulans*, were obtained from Mianwali, Pakistan (32.5839° N, 71.5370° E). The leaf samples were rinsed with 70% ethanol, and total genomic DNA was extracted, following the CTAB (cetyltrimethylammonium bromide) method [31]. DNA quality and concentration were assessed by Colibri spectrometer Nanodrop Titertek-Berthold, Berthold Detection Systems GmbH, Pforzheim, Germany) and 1% agarose gel electrophoresis. The genome was sequenced, using the Illumina HiSeq PE150 platform (Illumina Inc., San Diego, CA, USA) (Beijing Institute of Genomics). Furthermore, the Illumina sequence data of *W. adpressa* (5 Gb) and *W. riebeckii* (5 Gb) were acquired from the Sequence Read Archive (SRA) deposited under accession numbers SRR8718119 and SRR8718120. The raw sequencing read quality was checked with the FastQC tool [32]. We used Velvet 1.2.10 [33] with k-mer sizes of 71, 91, 101, and 111 to initially assemble the large sequence contigs from raw paired-end reads. Then, using the *de novo* assembly option of Geneious R8.1 (Biomatters Ltd., Auckland, New Zealand [34], these contigs were combined to produce complete plastid genomes. The junction sites between LSC, SSC, and IR were determined for these novel assembled plastomes. Annotations of the genome sequence were performed, using GeSeq [35] and CPGAVAS2 [36]. Then, the results were compared, inspected, and curated manually. Additionally, tRNA genes were identified, using tRNAscan-SE version 2.0 under default parameters [37] and Aragorn version 1.2.38 [38]. CPGAVAS2 [36] and Clico FS [39] was used to draw circular maps of the genomes. The average coverage depths of the *Withania* species plastomes were determined by mapping the reads to the *de novo* assembled plastid genome through the Burrows-Wheeler Aligner (BWA) [40] and visualizing in Tablet [41].

The novel annotated plastid genomes were deposited in the National Center for Biotechnology Information (NCBI) under the following accession numbers: *W. coagulans* (MN216390), *W. adpressa* (BK010847), and *W. riebeckii* (BK010849), while the plastid genome of *W. coagulans* was also deposited in the GWH database of the National Genomics Data Center [42] with the accession number GWHACBF000000000.

### Comparative chloroplast genome analysis

All *de novo* plastid genomes were aligned with Multiple Alignment using Fast Fourier Transform (MAFFT) 7.309 [43], using default parameters, while protein-encoding genes, intergenic spacer (IGS) regions, and introns were extracted to analyze nucleotide diversity in DnaSP v6 [44]. The substitution and transition (Ts) and transversion (Tv) rates were resolved from the MAFFT alignment, using *W. somnifera* as a reference for the other *Withania* species. Each structural element, including the LSC, SSC, and IR, was aligned individually, and SNPs and InDel polymorphisms were analyzed in DnaSP. The expansion and contraction of IRs and their border positions were compared among *Withania* species, using IRscope [45]. To analyze the structural evolution of *Withania* plastid genome, the four genome sequences were compared using Circoletto [46] combining blastn search (e-value of  $<1 \times 10^{-10}$ ) with Circos output.

Potential RNA editing sites were predicted, using Predictive RNA Editor for Plants-chloroplast genes (PREP-cp) and default settings [47], while the relative synonymous codon usage (RSCU) and amino-acid frequencies were analyzed in Geneious R8.1. The ratios of synonymous ( $K_s$ ) and non-synonymous ( $K_a$ ) substitutions for each extracted protein-encoding gene were calculated with DnaSP for all *Withania*, using *W. somnifera* as reference.

Microsatellite repeats in *Withania* plastid genomes were detected with MicroSAtellite-web (MISA) [48], using a minimal repeat number of 7 for mononucleotide simple sequence repeats (SSRs), four repeat units for dinucleotide SSRs, and three repeat units for tri-, tetra-, penta-, and hexanucleotide SSRs. We also used REPuter [49] with parameters: minimal repeat size 30 base pairs (bp), Hamming distance 3, minimum similarity percentage of two repeat copies 90%, maximum computed repeats numbers 500 bp for scanning and visualizing forward (F), reverse (R), palindromic (P), and complementary (C) repeats. Tandem repeats were also searched, using the tandem repeat finder program with default parameters [50].

## Plastid phylogenomic analysis

We included all available *Withania* plastid genome sequences in our analysis and added further Solanaceae plastid genomes (Organelle Genome Resources of NCBI, accessed on 21 January, 2020) from closely related groups of Physaleae and additional taxonomic groups from the so-called ‘x = 12 clade’ that encompasses the species from Solanoideae and Nicotianoideae. We used *Petunia × atkinsiana* (Sweet) D. Don ex W.H. Baxter (Syn.: *Petunia × hybrida* Vilm.) as an outgroup to root our tree, since this was the only available complete plastid genome sequence outside the x = 12 clade. For phylogenetic analysis, we removed one of the IR regions, and subsequently all protein-encoding genes were excised from the plastid genomes. The reading frames were manually verified during extraction by checking the start and stop codons. We discarded *accD*, *ycf1*, and *ycf15* from our final alignment, because these genes were highly variable in size. The trans-spliced *rps12* was also not included in the phylogenetic alignment together with sequence of the *infA* pseudogene. Sequences of 74 protein-coding genes were concatenated and aligned using MAFFT, then tree searches were performed in IQ-TREE 1.5.5 [51]. We used IQ-TREE to infer the best-fitting models of substitution for partitioning the matrix-combining multiple genes with the -TESTMERGEONLY and -AICc (Akaike information criterion corrected for small sample sizes) options in the built-in ModelFinder [52]. Maximum likelihood (ML) analyses were performed, using the ultrafast bootstrap approximation (UFBoot; [53]) with 1,000 replicates. The key idea behind UFBoot is to keep trees encountered during the ML-tree search for the original sequence alignment and to use them to evaluate the tree likelihoods for the bootstrap sequence alignment. UFBoot provides relatively unbiased bootstrap estimates under mild model misspecifications and reduces computing time while achieving more unbiased branch supports than standard bootstrap [53]. The SH-like approximate likelihood ratio test (SH-aLRT) was also conducted together with UFBoot, while TreeDyn was used for further enhancement of phylogenetic tree analysis [54,55].

## RESULTS

### Organization and characteristics of *Withania* plastid genomes

Our comparative analysis revealed that *Withania* species have similar plastid genome structures (Fig. 1 and Table 1). The length of the assembled plastid genomes varied between 154,198 bp and 154,361 bp. The average coverage depth of the assembled plastomes of *W. coagulans*, *W.*

*adpressa*, and *W. riebeckii* was 573×, 566×, and 590×, respectively. The total guanosine-cytosine (GC) content of the *de novo* assembled *Withania* plastid genomes was 37.7%, as was the previously sequenced species. The GC content of the IR region was higher (43.2%) than the LSC (35.7%) and SSC (31.8%) regions, which could have been due to the occurrence of rRNA genes, which are known to contain GC-rich regions [19, 55–58]. The plastomes of the *de novo* assembled *Withania* species had 132 unique genes, whereas 18 genes were duplicated in the IR (Table 2, Fig. 2). Out of these 132 genes, 86 were protein-encoding, 37 were tRNA, and 8 rRNA genes were similarly present in all species. The IR regions contained 18 duplicated genes and out of these 7 were protein-encoding, 4 were rRNA, and 7 were tRNA genes. The protein-encoding genes *clpP*, *ycf3*, and *rps12* contained two introns, while *rps16*, *atpF*, *rpoC1*, *petB*, *petD*, *rpl16*, *ndhA*, *rpl2*, and *ndhB* additional genes contained one intron each. The *rps12* gene was trans-spliced with its 5' end exon located in the LSC, while its two 3' end exons were found in the IR. The tRNAs (53%) and rRNAs (55.3%) showed the highest GC content. Hydrophobic amino acids were abundant, while the acidic amino acids were present in the least amount in plastid genomes of the genus *Withania*. These amino acids were adenine-thymine (AT)-rich sequences in all species (Fig. 3A). The RSCU and frequency of amino acids were also analyzed, which revealed that Leu is the most abundant, while cysteine (Cys) was the least encoded amino acid in *Withania* plastid genomes (Fig. 3B). The codon usage also revealed a shift towards the number of codons having A/T at the third position (Table S1).

### Divergence hotspots in *Withania*

Our comparison showed that all *Withania* genomes had similar nucleotide compositions in all structural (LSC, SSC, and IR) and coding regions, which extended even to IGSs (Table S2). The number of substitutions ranged between 28 and 110, while substitution types were shared among species (Table 3). The most frequently occurring mutations were A/G and C/T conversions, compared with other SNPs (Table 3). The ratio of Ts and Tv in the plastid genomes ranged from 1.09 to 1.2 in the LSC and between 0 and 1 in the SSC, while varying from 1 to 5 in the IR region (Table S3). In general, the Ts were more frequent in *Withania*, in line with observations in other plant species [59,60]. InDels were also examined, using DnaSP in all regions of the plastid genome. The number of InDels ranged from 42 to 44, mostly located in the LSC and sparsely found in the SSC, whereas the IRs contained only a few InDels (Table 4). This may have been due to the observation that IRs are more conserved in plastid genomes and evolve under concerted

evolution, while the LSC and SSC regions are more prone to substitutions [61]. In considering all positions with single- or multinucleotide variations as SNPs, then 205 SNPs were identified, corresponding to a mean SNP frequency of 0.2050 SNPs/kb in *Withania* species, while InDels showed a mean frequency of 0.128/kb.

The InDels and SNP mutational events in the plastid genome showed uneven distributions and clustered as 'hotspots' [62,63]. At this point, we chose 17 highly polymorphic regions for marker development (Table 5). Out of these 17 regions, 14 were IGSs, and 3 were genes. More polymorphism was shown in the IGS regions (average  $\pi = 0.6087$ ) than in the gene's regions ( $\pi = 0.3061$ ), intron (average  $\pi = 0.1061$ ), and exon (0.0439). Among the *Withania* species, the values ranged from 0 (*ycf4*) to 0.6122 (*ndhF* region) (Fig. 4). We further investigated the Ks and Ka substitutions and their ratio (Ka/Ks) among these hotspots (Table S4). We selected 77 protein-encoding genes for further analysis and found that 69 genes showed Ks = 0 and 58 had Ka = 0, while 72 genes had both Ks and Ka = 0. Of the protein-encoding genes, four (*accD*, *ycf2*, *ycf1*, *ndhF*) showed Ka/Ks ratios of more than 1, while *ycf1* and *psbC* showed Ka/Ks ratios greater than 0-1 for *W. riebeckii*, *ndhF* for *W. coagulans*, and *rps15* for *W. adpressa* and *accD*, *ycf2* showed had Ka/Ks greater than 0 for *W. adpressa* and *W. riebeckii* and *rpoC2* for *W. coagulans* and *W. riebeckii*. Most of the genes showed relatively slow evolutionary divergence, indicating the conserved nature of the protein-encoding genes found in the plastid genome. Plastid genes are mostly subjected to purifying selection, and the low Ka/Ks ratio is due to conservation of the functions of the photosynthetic apparatus.

### Repeat structure and analyses

Repeats in the plastid genome are useful in evolutionary studies and play crucial roles in genome arrangement, plant breeding, and linkage map construction [64–66]. We performed a microsatellite analysis that revealed shared microsatellite loci ranging from 376 (*W. coagulans*) to 379 (*W. adpressa*). Most SSRs were mononucleotide stretches followed by trinucleotide and dinucleotide repeats. In these groups, A/T motifs were highly abundant in mononucleotides, and AT/TA motifs were frequently observed among dinucleotide SSRs. The mononucleotide SSR motifs varied from 7- to 17-unit repeat; in dinucleotide SSRs, the motif change was from 4- to 5-unit repeats, whereas other types of SSRs were present mainly in 3--5-unit repeats. Most SSRs occurred in the LSC, followed by IR and SSC (Fig. 5) (Table S5). REPuter was also employed to locate further tandem

repeats in all *Withania* species. A total of 66 oligonucleotide repeats were found among *Withania* species. The F and P repeats were present in large numbers in all species. The oligonucleotide repeats were variable in size (30-60 bp) and a large fraction of the repeats was located in the LSC and existed in IGS regions, followed by gene, intron, and coding DNA sequence (CDS) regions (Fig. 6) (Table S7). The number of tandem repeats varied from 22 to 25 between *Withania* species (Fig. 7) (Table S6).

### **Comparative plastomics and inverted repeat boundaries**

The plastid genome of land plants has a conserved quadripartite structure, but diversity exists at the junction sites of the major structural regions of the genome. The variations in plastid genome sizes can also be attributed to changes in the IR structure, such as contractions and expansions or even loss of IRs along with the changes in the length of IGSs [67,68]. The size range of LSC, SSC, and IR varies among the plastid genomes of the species, which may progress to alterations in several genes, leading to deletion, duplication, or functional pseudogenization at the junction sites. The variations at the joining sites of different regions of the plastid genome can help to expand our knowledge of the evolution of species [68]. Liu et al. [69] reported that the similarities at the joining regions may be used to explain the relationship between the species, while those plants having high levels of relatedness show minimal fluctuations at the junctions of the cp genome. To investigate such events, we compared the JL (LSC/IR) and JS (IR/SSC) junction sites of *Withania* plastid genomes (Fig. 8). The resemblance at junctions revealed the close resemblance among the *Withania* species. The *rps19* gene was found at the junction site of JLB (LSC/IRb), and a portion of this gene (8-59 bp) was copied in the IRa in all *Withania* genomes. The *ndhF* gene was entirely present in the SSC region in *W. somnifera* and *W. adpressa*, but in *W. coagulans* (5 bp) and *W. riebeckii* (3 bp) it was located in the IRb region.

### **Putative RNA-editing sites**

RNA editing can modify the DNA-encoded sequencing of transcribed RNA by adding, deleting, or modifying the nucleotides [46]. RNA editing aids in creating transcripts and maintaining protein diversity [70]. Some RNA-editing sites in plastomes are conserved in higher plants [71]. To examine the RNA editing in *Withania* species, we predicted putative sites in the plastid genomes, using PREP-cp which revealed 37 putative sites in 15 genes of *W. somnifera* while 35, 39, and 37 editing sites were found in 13 genes of *W. coagulans*, and 14 genes of *W. adpressa*, and *W.*

*riebeckii*, respectively. The gene *clpP* has editing sites only in *W. somnifera* and *ccsA* only in *W. adpressa*. Most of these RNA-editing sites were found among *ndhB* (9), *ndhD* (7), and *rpoB* (5). All *Withania* species have high levels of conversion for Serine (Ser) to Leucine (Leu) 60%, 53.8%, and 59.4%, respectively, followed by Proline (Pro) to Leu 14.28%, 17.94%, and 16.21%, respectively and Ser to Phenylalanine (Phe) 8.57%, 10.2%, and 10.8%, respectively. Of the putative RNA-editing sites detected 33 (94.2%), 34 (87.1%), and 33 (89.1%) codons substituted on the second nucleotide and 2 (5.71%), 5 (12.8%), and 4 (10.81%) codons substituted on the first nucleotide in *W. coagulans*, *W. adpressa*, and *W. riebeckii*. Many amino acids were converted from Ser to Leu and changes at these sites assisted in the formation of hydrophobic amino acids, e.g. Valine (Val), Leu and Phe (Table S8).

### Phylogenetic Analysis

We performed maximum-likelihood analysis for phylogenetic reconstruction for 19 Solanaceae species, based on selected protein-coding gene sequences extracted from whole-plastid genome sequences. Our tree was reconstructed, based on a 69,582-bp alignment, and resolved a phylogenetic tree supported by high bootstrap values (Fig. 9). The genus *Withania* was represented by *W. adpressa*, native to North Africa, Morocco, and Algeria, *W. coagulans* from the eastern distribution area, *W. riebeckii* native to the island of Socotra, Jemen, and finally, the widespread *W. somnifera*. Our phylogenetic analysis of the genus *Withania* showed that it is monophyletic and closely related to groundcherries (*Physalis* L.), with which it is often confused, and like the latter also belongs to the subfamily Solanoideae. However, this relationship needs further sampling to investigate the relationship of the allied genera. Our results were consistent with results from the plastid intergenic *atpB-rbcL* spacer [71] *ndhF* and *trnLF* [1] and also based on whole-plastid genome sequences [18].

### DISCUSSION

Chloroplast DNA (cpDNA) is an excellent source of molecular variation available for higher-order (i.e. generic level and above) phylogenetic studies in plants [19,66,73]. Data from the study of cpDNA have helped to resolve some long-standing problems in Solanaceae systematics [74]. Thus, we characterized, annotated, and analyzed the plastid genome of *Withania* species which was further used in phylogenetic inference. *Withania* species belong to a rather diverse and widely distributed Withaninae clade within the so-called physaloid group. Species of the genus *Withania*

are morphologically similar: the flowers are found in axillary fascicles with the peduncle absent. The corollas are campanulate, urceolate, rotate, or salverform, while the filaments are often with conspicuous lateral appendages, forming nectar grooves. The Withaninae clade consists of approximately seven small often monotypic genera, such as *Tubocapsicum* (Wettst.) Makino, *Mellissia* Hook. f., *Aureliana* Sendtn. or *Discopodium* Hochst., which are herbs, shrubs, or trees primarily from the Old World. D’Arcy [75] considered *Withania* to be one of the truly Old-World genera, while Symon [76] regarded it as a distinctive African Gondwanan element. *Withania* has two centers of distribution: the first, located in the Canary Islands, Spain, and Northwest Africa and the second, in the Horn of Africa, South Arabia, and India. The phylogenetic relationships within the genus are poorly known, and the biology, chromosome numbers, and the exact number of species are also lacking. Chromosome counts showed that most species of *Withania* are polyploids with  $2n = 2x = 48$  [77], derived from the  $x = 12$  haploid chromosome number typical for the majority of Solanaceae species. In addition to the currently accepted *Withania* taxa, there are 35 unresolved botanical names that need further investigation to clarify the taxonomy of the genus.

In Hepper’s treatment [78], *Withania* consisted of 10 species, which were extended by Hunziker [79] with the addition of nine mesophytes from the genera *Mellissia* Hook. and *Physaliastrum* Makino. These additions extended the geographical range of the genus from the Canary Islands in the west, through Asia to China and Japan in the east. Symon [75] also emphasized the similarity of *Mellissia* (a critically endangered endemic of St Helena) to *Withania* but retained them as distinct genera. In contrast, Hunziker [79] included *Mellissia* within *Withania* and molecular results support this placement [1]. There is no consensus on the positions of the small clades related to *Withania*, while its closest relatives are also debated. In our analysis, *Withania* resembles *Physalis*, which is similar to the results of Deanna et al. [77], although this branching is supported by only weak bootstrap values.

Plastid genome sequences could be used as tools to further elucidate species boundaries and investigate the phylogenetic relationships among the small clades of Withaninae and resolve the taxonomic debate over the placement of *Melissia* and other monotypic genera. For such barcoding studies our results could provide valuable reference genomes for assemblies. The hotspot regions described in our study could be useful in such phylogenetic or even population genetic investigations. It was previously demonstrated that identifying highly variable regions by

comparative plastomics could provide crucial information about the loci suitable for development of molecular markers [57,80–82]. Such divergent hotspots in the plastomes can be applied for DNA barcoding at the generic level [29,83–85]. Thus, the set of 30 polymorphic regions identified among *Withania* in our study could be applied for DNA barcoding.

By further analyzing the Ks and Ka arrangement of nucleotide substitution of these divergent hotspots, we observed that the Ks substitutions are greater relative to the Ka substitutions. Such observations are essential markers in evolution for defining slow- and fast-evolving genes [86]. The ratio of Ka/Ks also informs us about the selection pressure on these genes. When the Ka/Ks value is minimal, it represents purifying selection, while values similar to it or equal to 1 represent neutral evolution, and values greater than 1 denote positive selection [85]. Most plastid genes showed a minimal Ka/Ks ratio (< 0.5), demonstrating that purifying selection is acting over these genes, due to functional constraints of the plastid genome. However, *atpB*, *ndhD*, *ndhF*, *rpoA*, *rpoC1*, *rps2*, and *rps12* showed greater Ka/Ks values (> 1), possibly indicating selective pressure acting over these genes that was previously proposed in other groups [57,87–89]. Our sampling in the *Withania* clade was limited to further explore the biological causes of the elevated Ka/Ks ratios observed in cases involving these genes. Here, we suggest that the following set of genes could be the principal candidates in investigations of these environmental interactions and their effects on plastid genes. Such investigations should include a nearly complete phylogenetic sampling of *Withania* and consider the random fluctuations in Ka and Ks estimates that could easily lead to erroneous inferences. Random fluctuations in the underlying sequences or in their sampling can easily shift the inference of Ka and Ks to above 1, leading to an inferred positively selected inference. This shortcoming can be bypassed by complete sampling and additional tests of selective pressure.

## CONCLUSIONS

Here, we sequenced, assembled, annotated, and compared the complete plastid genome sequence of three *Withania* species. The structure of these genomes showed organization similar to that previously reported for species of the Solanaceae. We identified sequence divergence hotspots and located repeat sequences and InDels in the plastomes of *Withania* species. These regions may constitute a useful means to develop suitable molecular markers for species identification and DNA barcoding of ashwagandha medicinal products. Such commonly used herbal products are

frequently bundled by the industry as formulated raw herbs collected in the wild and transported to international markets. The long transportation chain, with many middlemen, results in increased events of misidentification and adulteration [90]. Due to lack of proper monitoring and regulatory systems, there is a risk that many medicinal plants and their products sold on the market will be taxonomically misidentified, mislabeled, or contaminated [90]. Globally, the focus has been on the potential hazards of traditional herbal medicinal products [91]. It is hoped that our study will aid in the development of DNA-barcoding markers to clarify the taxonomic identity of *Withania* species in medicinal plant production. Plastid genome-based ‘superbarcoding’ is repeatable, reliable, and sensitive enough to distinguish look-alike species and has the potential for becoming a valuable tool for the biomonitoring of multi-ingredients manufactured from ashwagandha.

### Acknowledgements

This work was supported by the National Key Research and Development Program of China [2016YFE0206600 to Y.B.]; The 13th Five-year Informatization Plan of the Chinese Academy of Sciences [XXH13505–05 to Y.B.]; The 100-Talent Program of the Chinese Academy of Sciences [to Y.B.]; The Open Biodiversity and Health Big Data Initiative of IUBS [to Y.B.]. We highly acknowledge the DNA4 Technologies LLC (*Withania adpressa*, *Withania riebeckii*) for sequencing and deposition of the raw sequencing data in the public repository of the National Center of Biotechnology Information. The authors thank James Thompson for editing the manuscript.

### Conflict of interest

The authors declare that they have no conflict of interest.

### References

1. Olmstead, R.G.; Bohs, L.; Migid, H.A.; Santiago-Valentin, E. Garcia, V.F.; Collier, S.M. A Molecular phylogeny of the Solanaceae. *Taxon* **2008**, *57*, 1159–1181.
2. Olmstead, R.G.; Bohs, L. A summary of molecular systematic research in solanaceae: 1982-2006. Solanaceae IV: Genomics meets biodiversity. Proceedings of the VIth international Solanaceae conference, Madison, Wisconsin, USA. 2007. pp 255–268
3. Knapp, S.; Bohs, L.; Nee, M.; Spooner, D.M. Solanaceae - A model for linking genomics with biodiversity. *Comp. Funct. Genomics* **2004**, *5*, 285–291.
4. Mirjalili, M.H.; Moyano, E.; Bonfill, M.; Cusido, R.M.; Palazón, J. Steroidal lactones from withania somnifera, an ancient plant for novel medicine. *Molecules* **2009**, *14*, 2373–2393.
5. Singh, P.; Guleri, R.; Singh, V.; Kaur, G.; Kataria, H.; Singh, B.; Kaur, G.; Kaul, S.C.;

- Wadhwa, R.; Pati, P.K. Biotechnological interventions in *Withania somnifera* (L.) Dunal. *Biotechnol. Genet. Eng. Rev.* **2015**, *31*, 1–20.
6. Uddin, Q.; Samiulla, L.; Singh, V.K.; Jamil, S.S. Phytochemical and pharmacological profile of *Withania somnifera* Dunal: A review. *J. Appl. Pharm. Sci.* **2012**, *2*, 170–175.
  7. Maurya, R. Chemistry and pharmacology of *Withania coagulans*: an Ayurvedic remedy. *J. Pharm. Pharmacol.* **2010**, *62*, 153–160.
  8. Ihsan-ul-Haq; Youn, U.J.; Chai, X.; Park, E.-J.; Kondratyuk, T.P.; Simmons, C.J.; Borris, R.P.; Mirza, B.; Pezzuto, J.M.; Chang, L.C. Biologically active withanolides from *Withania coagulans*. *J. Nat. Prod.* **2013**, *76*, 22–28.
  9. Rehman, S.; Keefover-Ring, K.; Haq, I. ul; Dilshad, E.; Khan, M.I.; Akhtar, N.; Mirza, B. Drier Climatic Conditions Increase Withanolide Content of *Withania coagulans* Enhancing Its Inhibitory Potential Against Human Prostate Cancer Cells. *Appl. Biochem. Biotechnol.* **2019**, *188*, 460–480.
  10. Shinwari, Z.K. Medicinal plants research in Pakistan. *J. Med. Plants Res.* **2010**, *4*, 161–176.
  11. Raclariu, A.C.; Heinrich, M.; Ichim, M.C.; de Boer, H. Benefits and Limitations of DNA Barcoding and Metabarcoding in Herbal Product Authentication. *Phytochem. Anal.* **2018**, *29*, 123–128.
  12. Li, M.; Cao, H.; But, P.P.H.; Shaw, P.C. Identification of herbal medicinal materials using DNA barcodes. *J. Syst. Evol.* **2011**, *49*, 271–283.
  13. Jin, S.; Daniell, H. The Engineered Chloroplast Genome Just Got Smarter. *Trends Plant Sci.* **2015**, *20*, 622–640.
  14. Cooper, G. *Chloroplasts and other plastids in the cell: A molecular approach. 2nd edition*; Sunderland, MA, Sinauer Associates, 2000.
  15. Palmer, J.D. Comparative organization of chloroplast genomes. *Annu. Rev. Genet.* **1985**, *19*, 325–354.
  16. Daniell, H.; Lin, C.-S.; Yu, M.; Chang, W.-J. Chloroplast genomes: diversity, evolution, and applications in genetic engineering. *Genome Biol.* **2016**, *17*, 134.
  17. Oldenburg, D.J.; Bendich, A.J. DNA maintenance in plastids and mitochondria of plants. *Front. Plant Sci.* **2015**, *6*, 883.
  18. Amiryousefi, A.; Hyvönen, J.; Poczai, P. The chloroplast genome sequence of bittersweet (*Solanum dulcamara*): Plastid genome structure evolution in Solanaceae. *PLoS One* **2018**, *13*, 1–23.
  19. Abdullah; Shahzadi, I.; Mehmood, F.; Ali, Z.; Malik, M.S.; Waseem, S.; Mirza, B.; Ahmed, I.; Waheed, M.T. Comparative analyses of chloroplast genomes among three *Firmiana* species: Identification of mutational hotspots and phylogenetic relationship with other species of Malvaceae. *Plant Gene* **2019**, 100199.
  20. Jheng, C.-F.; Chen, T.-C.; Lin, J.-Y.; Chen, T.-C.; Wu, W.-L.; Chang, C.-C. The comparative chloroplast genomic analysis of photosynthetic orchids and developing DNA markers to distinguish *Phalaenopsis* orchids. *Plant Sci.* **2012**, *190*, 62–73.
  21. Xu, J.-H.; Liu, Q.; Hu, W.; Wang, T.; Xue, Q.; Messing, J. Dynamics of chloroplast

- genomes in green plants. *Genomics* **2015**, *106*, 221–231.
22. Moore, M.J.; Bell, C.D.; Soltis, P.S.; Soltis, D.E. Using plastid genome-scale data to resolve enigmatic relationships among basal angiosperms. *Proc. Natl. Acad. Sci.* **2007**, *104*, 19363–19368.
  23. Ravi, V.; Khurana, J.P.; Tyagi, A.K.; Khurana, P. An update on chloroplast genomes. *Plant Syst. Evol.* **2008**, *271*, 101–122.
  24. Yang, M.; Zhang, X.; Liu, G.; Yin, Y.; Chen, K.; Yun, Q.; Zhao, D.; Al-Mssallem, I.S.; Yu, J. The complete chloroplast genome sequence of date palm (*Phoenix dactylifera* L.). *PLoS One* **2010**, *5*, e12762.
  25. Bi, Y.; Zhang, M.F.; Xue, J.; Dong, R.; Du, Y.P.; Zhang, X.H. Chloroplast genomic resources for phylogeny and DNA barcoding: A case study on *Fritillaria*. *Sci. Rep.* **2018**, *8*, 1184.
  26. Bansal, K.C.; Saha, D. Chloroplast Genomics and Genetic Engineering for Crop Improvement. *Agric. Res.* **2012**, *1*, 53–66.
  27. Waheed, M.T.; Thönes, N.; Müller, M.; Hassan, S.W.; Razavi, N.M.; Lössl, E.; Kaul, H.P.; Lössl, A.G. Transplastomic expression of a modified human papillomavirus L1 protein leading to the assembly of capsomeres in tobacco: A step towards cost-effective second-generation vaccines. *Transgenic Res.* **2011**, *20*, 271–282.
  28. Waheed, M.T.; Ismail, H.; Gottschamel, J.; Mirza, B.; Lössl, A.G. Plastids: The Green Frontiers for Vaccine Production. *Front. Plant Sci.* **2015**, *6*, 1005.
  29. Ahmad, I. Evolutionary dynamics in taro, Massey University, Palmerston North, New Zealand, 2014.
  30. Wambugu, P.W.; Brozynska, M.; Furtado, A.; Waters, D.L.; Henry, R.J. Relationships of wild and domesticated rices (*Oryza* AA genome species) based upon whole chloroplast genome sequences. *Sci. Rep.* **2015**, *5*, 13957.
  31. Murray, M.G.; Thompson, W.F. Rapid isolation of high molecular weight plant DNA. *Nucleic Acids Res.* **1980**, *8*, 4321–4325.
  32. Andrews, S. FASTQC. A quality control tool for high throughput sequence data. Available: <https://www.bioinformatics.babraham.ac.uk/projects/fastqc/> (accessed on 14.02.2020)
  33. Zerbino, D.R.; Birney, E. Velvet: Algorithms for de novo short read assembly using de Bruijn graphs. *Genome Res.* **2008**, *18*, 821–829.
  34. Kearse, M.; Moir, R.; Wilson, A.; Stones-Havas, S.; Cheung, M.; Sturrock, S.; Buxton, S.; Cooper, A.; Markowitz, S.; Duran, C.; et al. Geneious Basic: An integrated and extendable desktop software platform for the organization and analysis of sequence data. *Bioinformatics* **2012**, *28*, 1647–1649.
  35. Tillich, M.; Lehwark, P.; Pellizzer, T.; Ulbricht-Jones, E.S.; Fischer, A.; Bock, R.; Greiner, S. GeSeq – versatile and accurate annotation of organelle genomes. *Nucleic Acids Res.* **2017**, *45*, W6–W11.
  36. Shi, L.; Chen, H.; Jiang, M.; Wang, L.; Wu, X.; Huang, L.; Liu, C. CPGAVAS2, an

- integrated plastome sequence annotator and analyzer. *Nucleic Acids Res.* **2019**, *47*, W65–W73.
37. Lowe, T.M.; Chan, P.P. tRNAscan-SE On-line: integrating search and context for analysis of transfer RNA genes. *Nucleic Acids Res.* **2016**, *44*, W54–W57.
  38. Laslett, D.; Canback, B. ARAGORN, a program to detect tRNA genes and tmRNA genes in nucleotide sequences. *Nucleic Acids Res.* **2004**, *32*, 11–16.
  39. Cheong, W-H.; Tan, Y-C.; Yap, S-J; Ng, K-P. Clico FS: an interactive web-based service of Circos. *Bioinformatics* **2015**, *31*, 3685–3687.
  40. Li, H.; Durbin, R. Fast and accurate short read alignment with Burrows-Wheeler transform. *Bioinformatics* **2009**, *25*, 1754–1760.
  41. Milne, I.; Bayer, M.; Cardle, L.; Shaw, P.; Stephen, G.; Wright, F.; Marshall, D. Tablet-next generation sequence assembly visualization. *Bioinformatics* **2009**, *26*, 401–402.
  42. Zhang, Z.; Zhao, W.; Xiao, J.; Bao, Y.; He, S.; Zhang, G.; Li, Y.; Zhao, G.; Chen, R.; Gao, Y.; et al. Database Resources of the National Genomics Data Center in 2020. *Nucleic Acids Res.* **2019**, *48*, D24–D33.
  43. Katoh, K.; Kuma, K.I.; Toh, H.; Miyata, T. MAFFT version 5: Improvement in accuracy of multiple sequence alignment. *Nucleic Acids Res.* **2005**, *33*, 511–518.
  44. Rozas, J.; Ferrer-Mata, A.; Sanchez-DelBarrio, J.C.; Guirao-Rico, S.; Librado, P.; Ramos-Onsins, S.E.; Sanchez-Gracia, A. DnaSP 6: DNA sequence polymorphism analysis of large data sets. *Mol. Biol. Evol.* **2017**, *34*, 3299–3302.
  45. Amiryousefi, A.; Hyvönen, J.; Poczai, P. IRscope: an online program to visualize the junction sites of chloroplast genomes. *Bioinformatics* **2018**, *34*, 3030–3031.
  46. Darzentas, N. Circoletto: visualizing sequence similarity with Circos. *Bioinformatics* **2010**, *26*, 2620–2621
  47. Mower, J.P. The PREP suite: Predictive RNA editors for plant mitochondrial genes, chloroplast genes and user-defined alignments. *Nucleic Acids Res.* **2009**, *37*, W253–W259.
  48. Beier, S.; Thiel, T.; Münch, T.; Scholz, U.; Mascher, M. MISA-web: a web server for microsatellite prediction. *Bioinformatics* **2017**, *33*, 2583–2585.
  49. Kurtz, S. Choudhuri, J.V.; Ohlebusch, E.; Schleiermacher, C.; Stoye, J.; Giegerich, R. REPuter: the manifold applications of repeat analysis on a genomic scale. *Nucleic Acids Res.* **2002**, *29*, 4633–4642.
  50. Benson, G. Tandem repeats finder: A program to analyze DNA sequences. *Nucleic Acids Res.* **1999**, *27*, 573–580.
  51. Nguyen, L.-T.; Schmidt, H.A.; von Haeseler, A.; Minh, B.Q. IQ-TREE: A fast and effective stochastic algorithm for estimating Maximum-likelihood phylogenies. *Mol. Biol. Evol.* **2015**, *32*, 268–274.
  52. Kalyaanamoorthy, S.; Minh, B.Q.; Wong, T.K.F.; von Haeseler, A.; Jermini, L.S. ModelFinder: fast model selection for accurate phylogenetic estimates. *Nat. Methods* **2017**, *14*, 587–589.

53. Hoang, D.T.; Chernomor, O.; von Haeseler, A.; Minh, B.Q.; Vinh, L.S. UFBoot2: Improving the ultrafast bootstrap approximation. *Mol. Biol. Evol.* **2018**, *35*, 518–522.
54. Dereeper, A.; Guignon, V.; Blanc, G.; Audic, S.; Buffet, S.; Chevenet, F.; Dufayard, J.-F.; Guindon, S.; Lefort, V.; Lescot, M.; et al. Phylogeny.fr: robust phylogenetic analysis for the non-specialist. *Nucleic Acids Res.* **2008**, *36*, W465–W469.
55. Lemoine, F.; Correia, D.; Lefort, V.; Doppelt-Azeroual, O.; Mareuil, F.; Cohen-Boulakia, S.; Gascuel, O. NGPhylogeny.fr: new generation phylogenetic services for non-specialists. *Nucleic Acids Res.* **2019**, *47*, W260–265.
56. Qian, J.; Song, J.; Gao, H.; Zhu, Y.; Xu, J.; Pang, X.; Yao, H.; Sun, C.; Li, X.; Li, C.; et al. The complete chloroplast genome sequence of the medicinal plant *Salvia miltiorrhiza*. *PLoS One* **2013**, *8*, e57607.
57. Abdullah; Mehmood, F.; Shahzadi, I.; Waseem, S.; Mirza, B.; Ahmed, I.; Waheed, M.T. Chloroplast genome of *Hibiscus rosa-sinensis* (Malvaceae): Comparative analyses and identification of mutational hotspots. *Genomics* **2020**, *112*, 581–591.
58. Shahzadi, I.; Abdullah; Mehmood, F.; Ali, Z.; Ahmed, I.; Mirza, B. Chloroplast genome sequences of *Artemisia maritima* and *Artemisia absinthium*: Comparative analyses, mutational hotspots in genus *Artemisia* and phylogeny in family Asteraceae. *Genomics* **2019**. DOI: <https://doi.org/10.1016/j.ygeno.2019.08.016>
59. Song, Y.; Chen, Y.; Lv, J.; Xu, J.; Zhu, S.; Li, M. Comparative Chloroplast Genomes of *Sorghum* Species: Sequence Divergence and Phylogenetic Relationships. *BioMed Res. Int.* **2019**, DOI: <https://doi.org/10.1155/2019/5046958>
60. Sun, J.; Chen, M.; Yujiang; Zhao, D.; Tao, J. Characterization of the Complete Chloroplast Genomes of Sequences of Two Diploid Species: *Paeonia lactiflora* ‘Da Fugui’ and *Paeonia ostii* ‘Fengdan’ in the Paeoniaceae Family. *J. Hortic.* **2018**, *5*, 4.
61. Ahmed, I.; Biggs, P.J.; Matthews, P.J.; Collins, L.J.; Hendy, M.D.; Lockhart, P.J. Mutational dynamics of aroid chloroplast genomes. *Genome Biol. Evol.* **2012**, *4*, 1316–1323.
62. Shaw, J.; Lickey, E.B.; Schilling, E.E.; Small, R.L. Comparison of whole chloroplast genome sequences to choose noncoding regions for phylogenetic studies in angiosperms: The Tortoise and the hare III. *Am. J. Bot.* **2007**, *94*, 275–288.
63. Worberg, A.; Quandt, D.; Barniske, A.M.; Löhne, C.; Hilu, K.W.; Borsch, T. Phylogeny of basal eudicots: Insights from non-coding and rapidly evolving DNA. *Org. Divers. Evol.* **2007**, *7*, 55–77.
64. Powell, W.; Morgante, M.; McDevitt, R.; Vendramin, G.G.; Rafalski, J.A. Polymorphic simple sequence repeats regions in chloroplast genomes: applications to the population genetics of pines. *Proc. Natl. Acad. Sci. U. S. A.* **1995**, *92*, 7759–7763.
65. Xue, J.; Wang, S.; Zhou, S.L. Polymorphic chloroplast microsatellite loci in *Nelumbo* (Nelumbonaceae). *Am. J. Bot.* **2012**, *99*, e240–e244.
66. Zhang, Y.; Du, L.; Liu, A.; Chen, J.; Wu, L.; Hu, W.; Zhang, W.; Kim, K.; Lee, S.-C.; Yang, T.-J.; et al. The Complete Chloroplast Genome Sequences of Five *Epimedium* Species: Lights into Phylogenetic and Taxonomic Analyses. *Front. Plant Sci.* **2016**, *7*, 306.

67. Wang, R.J.; Cheng, C.L.; Chang, C.C.; Wu, C.L.; Su, T.M.; Chaw, S.M. Dynamics and evolution of the inverted repeat-large single copy junctions in the chloroplast genomes of monocots. *BMC Evol. Biol.* **2008**, *8*, 36
68. Palmer, J.D.; Jansen, R.K.; Michaels, H.J.; Chase, M.W.; Manhart, J.R. Chloroplast DNA Variation and Plant Phylogeny. *Ann. Missouri Bot. Gard.* **1988**, *75*, 1180–1206.
69. Liu, H.; He, J.; Ding, C.; Lyu, R.; Pei, L.; Cheng, J.; Xie, L. Comparative Analysis of Complete Chloroplast Genomes of *Anemoclema*, *Anemone*, *Pulsatilla*, and *Hepatica* Revealing Structural Variations Among Genera in Tribe Anemoneae (Ranunculaceae). *Front. Plant Sci.* **2018**, *9*, 1–16.
70. Bundschuh, R.; Altmüller, J.; Becker, C.; Nürnberg, P.; Gott, J.M. Complete characterization of the edited transcriptome of the mitochondrion of *Physarum polycephalum* using deep sequencing of RNA. *Nucleic Acids Res.* **2011**, *39*, 6044–6055.
71. Zeng, W.H.; Liao, S.C.; Chang, C.C. Identification of RNA editing sites in chloroplast transcripts of *Phalaenopsis aphrodite* and comparative analysis with those of other seed plants. *Plant Cell Physiol.* **2007**, *48*, 362–368.
72. Jamil, I.; Qamarunnisa, S.; Azhar, A.; Shinwari, Z.K.; Ali, S.I.; Qaiser, M.; Jamil, I.; Al, E.T. Subfamilial relationships within Solanaceae as inferred from *atpB-rbcL* intergenic spacer. *Pak. J. Bot.* **2014**, *46*, 585–590.
73. Jansen, R.K.; Cai, Z.; Raubeson, L.A.; Daniell, H.; dePamphilis, C.W.; Leebens-Mack, J.; Muller, K.F.; Guisinger-Bellian, M.; Haberle, R.C.; Hansen, A.K.; et al. Analysis of 81 genes from 64 plastid genomes resolves relationships in angiosperms and identifies genome-scale evolutionary patterns. *Proc. Natl. Acad. Sci.* **2007**, *104*, 19369–19374.
74. Olmstead, R.G.; Sweere, J.A.; Spangler, R.E.; Bohs, L.; Palmer, J.D. Phylogeny and Provisional Classification of the Solanaceae Based on Chloroplast DNA. In *Solanaceae IV: Advances in biology and utilization*. Nee M., Symon, D.E., Lester, R.N., Jessop J.P. Ed. Royal Botanic Gardens, Kew, pp. 111–137.
75. D'Arcy, W.G. The Solanaceae since 1976, with a review of its biogeography. In *Solanaceae III: Taxonomy, Chemistry, Evolution*. Hawkes, J.G.; Lester, R.N.; Nee, M.; Estrada, N. Ed.; Royal Botanic Gardens, Kew, UK, 1991; pp. 75–138.
76. Symon, D.E. Gondwanan elements of the Solanaceae. In *Solanaceae III: taxonomy, chemistry, evolution*; Hawkes JG, Lester RN, Nee M, Estrada N. Royal Botanical Gardens, Kew, U., Ed.; 1991; pp. 139–150.
77. Deanna, R.; Smith, S.D.; Särkinen, T.; Chiarini, F. Patterns of chromosomal evolution in the florally diverse Andean clade Iochrominae (Solanaceae). *Perspect. Plant Ecol. Evol. Syst.* **2018**, *35*, 31–43
78. Hepper, F.N. Old World *Withania* (Solanaceae): a taxonomic review and key to the species. In *Solanaceae III: Taxonomy, chemistry, evolution.*; In: Hakes JG, Lester RN, Nee M, Estrada. N., Ed.; Royal Botanic Gardens, Kew, UK, 1991; pp. 211–228.
79. Hunziker, A.T. *Genera Solanacearum: The Genera of Solanaceae Illustrated, Arranged According to a New System*. Ruggell: ARG Gantner Verlag, 2001.
80. Choi, K.S.; Chung, M.G.; Park, S. The complete chloroplast genome sequences of three

- veroniceae species (Plantaginaceae): comparative analysis and highly divergent regions. *Front. Plant Sci.* **2016**, *7*, 1–8.
81. Li, Y.; Zhang, Z.; Yang, J.; Lv, G. Complete chloroplast genome of seven *Fritillaria* species, variable DNA markers identification and phylogenetic relationships within the genus. *PLoS One* **2018**, *13*, e0194613
  82. Menezes, A.P.A.; Resende-Moreira, L.C.; Buzatti, R.S.O.; Nazareno, A.G.; Carlsen, M.; Lobo, F.P.; Kalapothakis, E.; Lovato, M.B. Chloroplast genomes of *Byrsonima* species (Malpighiaceae): Comparative analysis and screening of high divergence sequences. *Sci. Rep.* **2018**, *8*, 1–12.
  83. Ahmed, I.; Matthews, P.J.; Biggs, P.J.; Naeem, M.; Mclenachan, P.A.; Lockhart, P.J. Identification of chloroplast genome loci suitable for high-resolution phylogeographic studies of *Colocasia esculenta* (L.) Schott (Araceae) and closely related taxa. *Mol. Ecol. Resour.* **2013**, *13*, 929–937.
  84. Dong, W.; Liu, J.; Yu, J.; Wang, L.; Zhou, S. Highly variable chloroplast markers for evaluating plant phylogeny at low taxonomic levels and for DNA barcoding. *PLoS One* **2012**, *7*, e35071
  85. Nguyen, V.B.; Park, H.-S.; Lee, S.-C.; Lee, J.; Park, J.Y.; Yang, T.-J. Authentication markers for five major *Panax* species developed via comparative analysis of complete chloroplast genome sequences; *J. Agric. Food Chem.* **2017**, *65*, 6298–6306
  86. Kimura, M. Model of effectively neutral mutations in which selective constraint is incorporated. *Proc. Natl. Acad. Sci.* **1979**, *76*, 3440–3444
  87. Lawrie, D.S.; Messer, P.W.; Hershberg, R.; Petrov, D.A. Strong Purifying Selection at Synonymous Sites in *D. melanogaster*. *PLoS Genet.* **2013**, *9*, e1003527
  88. Poczai, P.; Hyvönen, J. The complete chloroplast genome sequence of the CAM epiphyte Spanish moss (*Tillandsia usneoides*, Bromeliaceae) and its comparative analysis. *PLoS One* **2017**, *12*, e0187199
  89. Menezes, A.P.A.; Resende-Moreira, L.C.; Buzatti, R.S.O.; Nazareno, A.G.; Carlsen, M.; Lobo, F.P.; Kalapothakis, E.; Lovato, M.B. Chloroplast genomes of *Byrsonima* species (Malpighiaceae): Comparative analysis and screening of high divergence sequences. *Sci. Rep.* **2018**, *8*, 2210
  90. Zahra, N.B.; Shinwari, Z.K.; Qaiser, M. DNA barcoding: A tool for standardization of herbal medicinal products (HMPs) of Lamiaceae from Pakistan. *Pak. J. Bot.* **2016**, *48*, 2167–2174.
  91. Xin, T.; Xu, Z.; Jia, J.; Leon, C.; Hu, S.; Lin, Y.; Ragupathy, S.; Song, J.; Newmaster, S.G. Biomonitoring for traditional herbal medicinal products using DNA metabarcoding and single molecule, real-time sequencing. *Acta Pharm. Sin. B* **2018**, *8*, 488–497

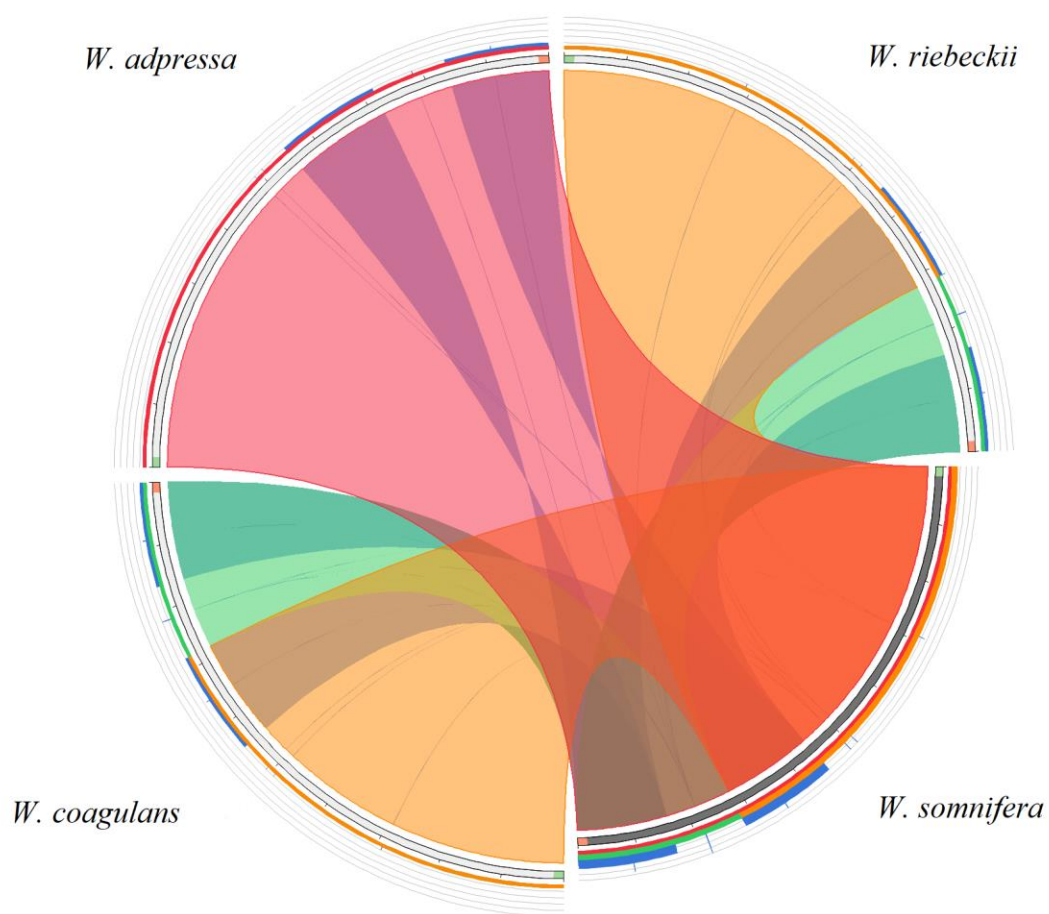


**Figure 1.** Structural comparison of *Withania* plastid genomes. Green and orange blocks in the beginning and end of sequences indicate the orientation of sequences. The colored blocks outside the sequences refer to the score/max bit core ration, with  $\leq 0.25$ , green  $\leq 0.50$ , orange  $\leq 0.75$ , and red  $> 0.75$ . Inverted repeat (IR) regions are represented by blue blocks.

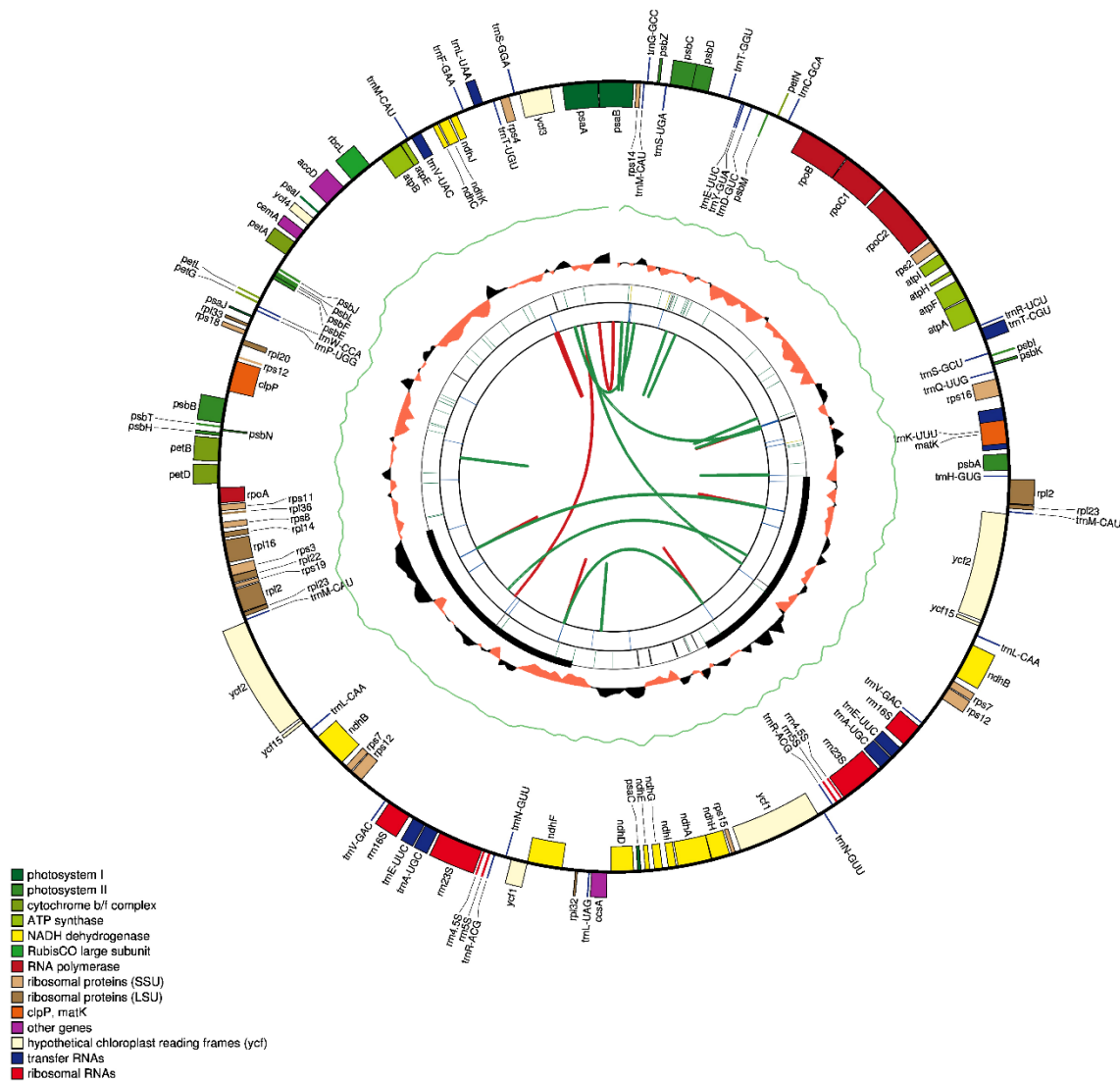


**Figure 2.** Gene maps of the plastomes of *Withania* species. From the center going outward, the first circle shows the forward and reverse repeats connected with red and green arcs respectively. The next circle shows the tandem repeats marked with short bars, while inverted repeat (IR) regions are represented by black bars. The third circle shows the microsatellite sequences identified using MISA. The fourth circle shows the gene structure on the plastid genome, where genes are colored based on their functional categories. GC content is plotted as a green line while a skewed GC plot is presented as an orange/black track around the inner circles.

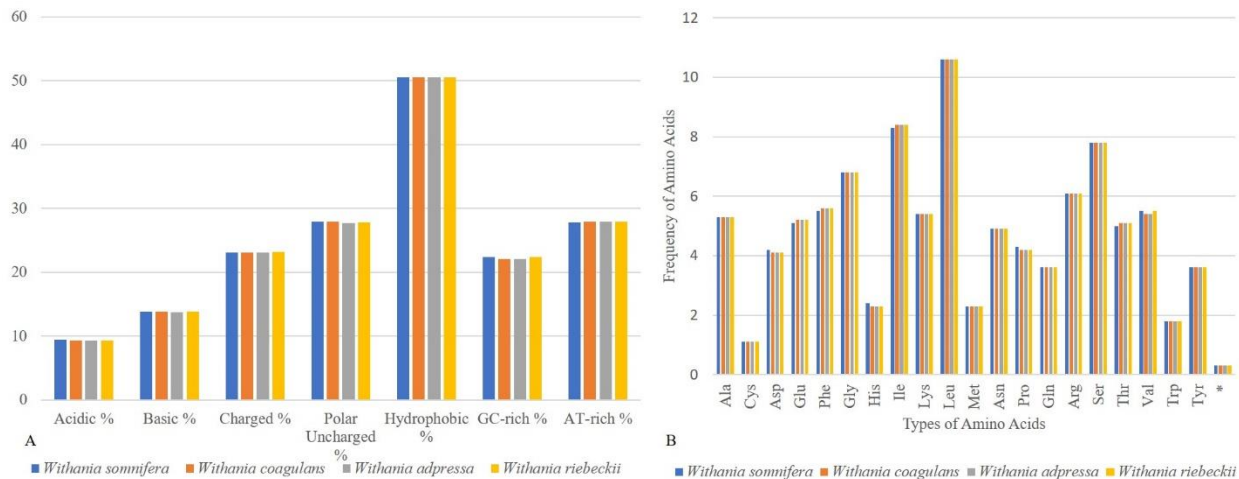


**Figure 3.** (A) Comparison of amino-acid groups and (B) Comparison of amino-acid frequency among *Withania*.

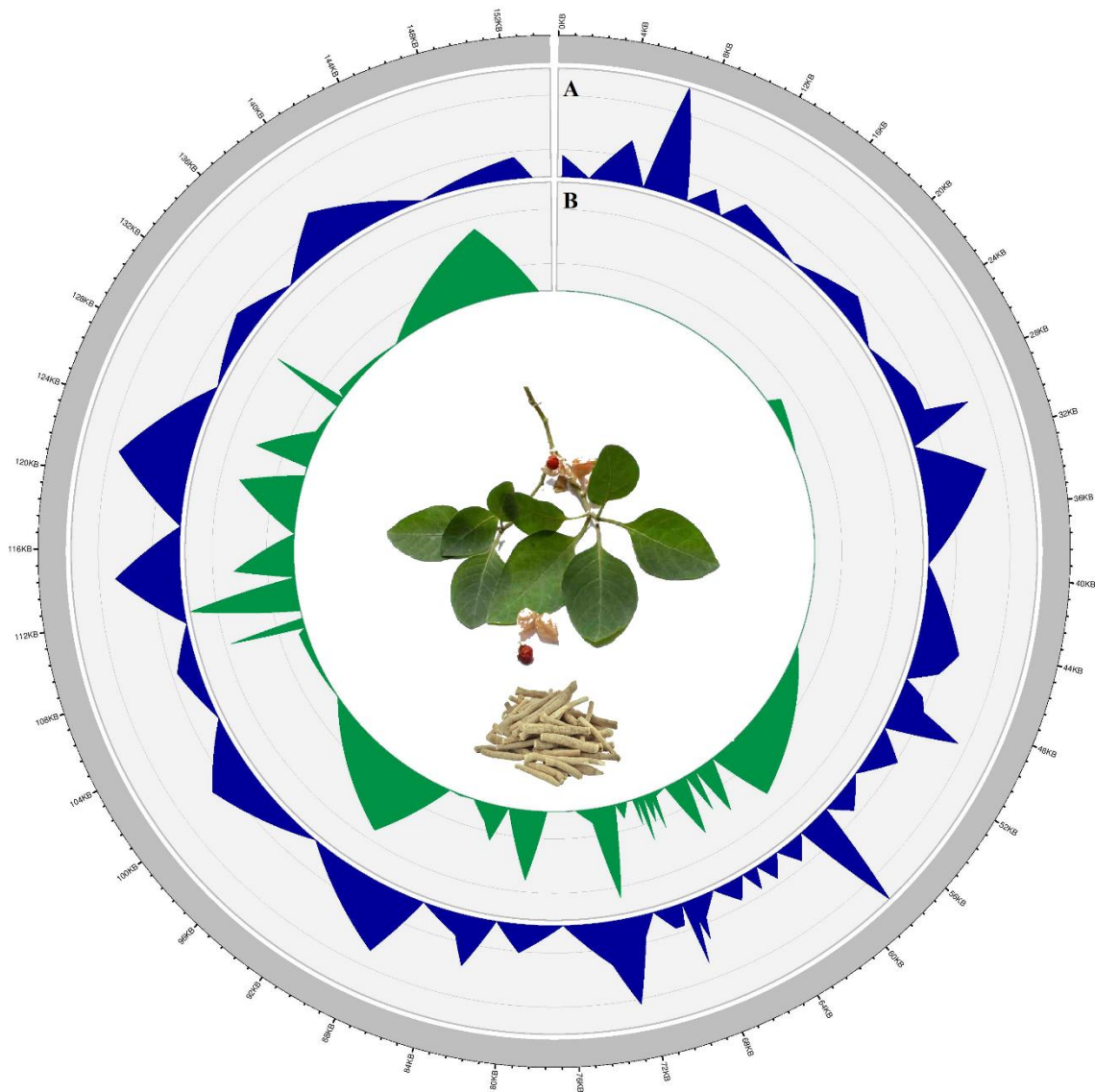


**Figure 4.** Indel (A) and nucleotide (B) diversity of various region of chloroplast genome among *Withania* species. The plastid genome is represented by a grey bar in a circle, while indel diversity is plotted as a blue (0 to 2.5) and nucleotide diversity as green (0 to 0.7) line graph.

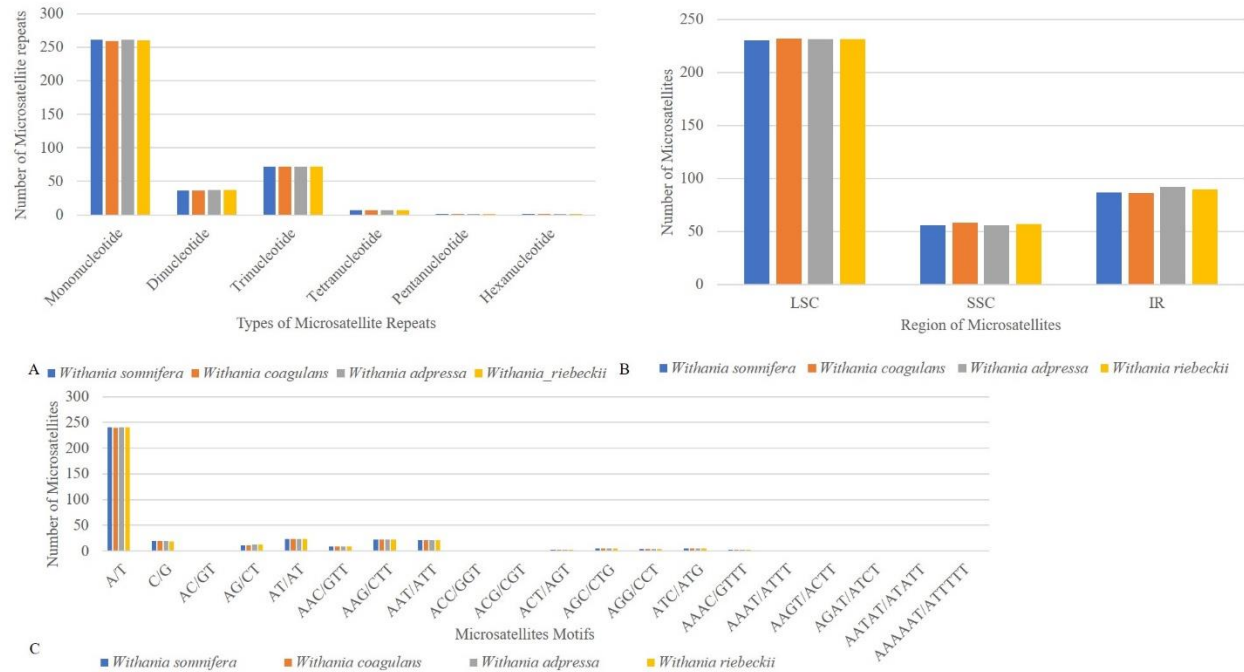


**Figure 5.** Comparative analysis of microsatellite repeats among *Withania* species (A) Indicates numbers of various types of microsatellite present in the *Withania* plastomes. (B) Distribution of simple sequence repeats (SSRs) in different regions (C) SSR motif distributions in different regions

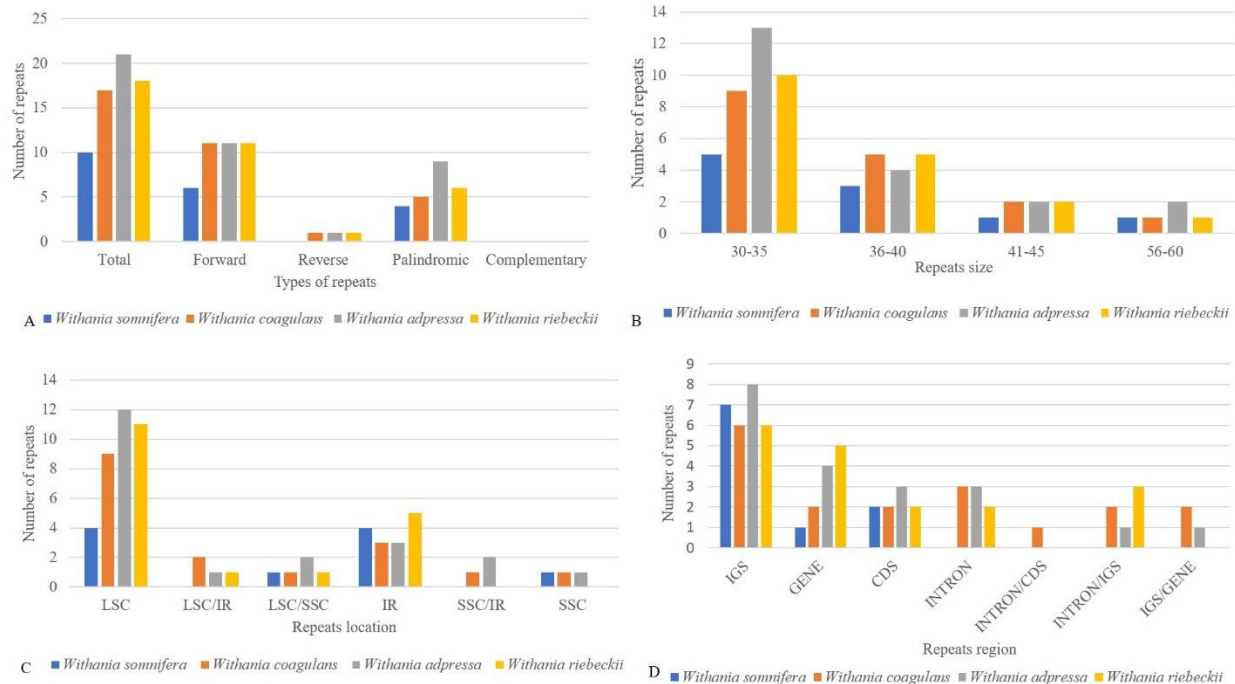


**Figure 6.** (A) Indicates various types of oligonucleotide repeats that exist in all *Withania* species (B) Indicates repeats that exist in ranges of size e.g. 30–35 indicates numbers of repeats within the size range that vary from 30 to 35 (C) Indicates numbers of repeats that exist in separate areas of the plastid genome. LSC: large single-copy, SSC: small single-copy, IR: inverted repeat region, LSC/SSC: one copy of LSC and another in SSC, LSC/IR: one copy of LSC and another in SSC, IR/SSC: one copy of IR and another in SSC, LSC/SSC/IR: one copy of LSC, one in SSC, and another in IR, (D) Indicates number of repeats in different regions of plastid genome, IGS: Intergenic spacer region, CDS: coding DNA sequences, Intron: intronic regions, IGS/Intron: one copy of the IGS region and another in intronic regions, Intron/CDS: one copy intron region and another in CDS regions, IGS/CDS: IGS region copy of repeat and one more in coding regions.

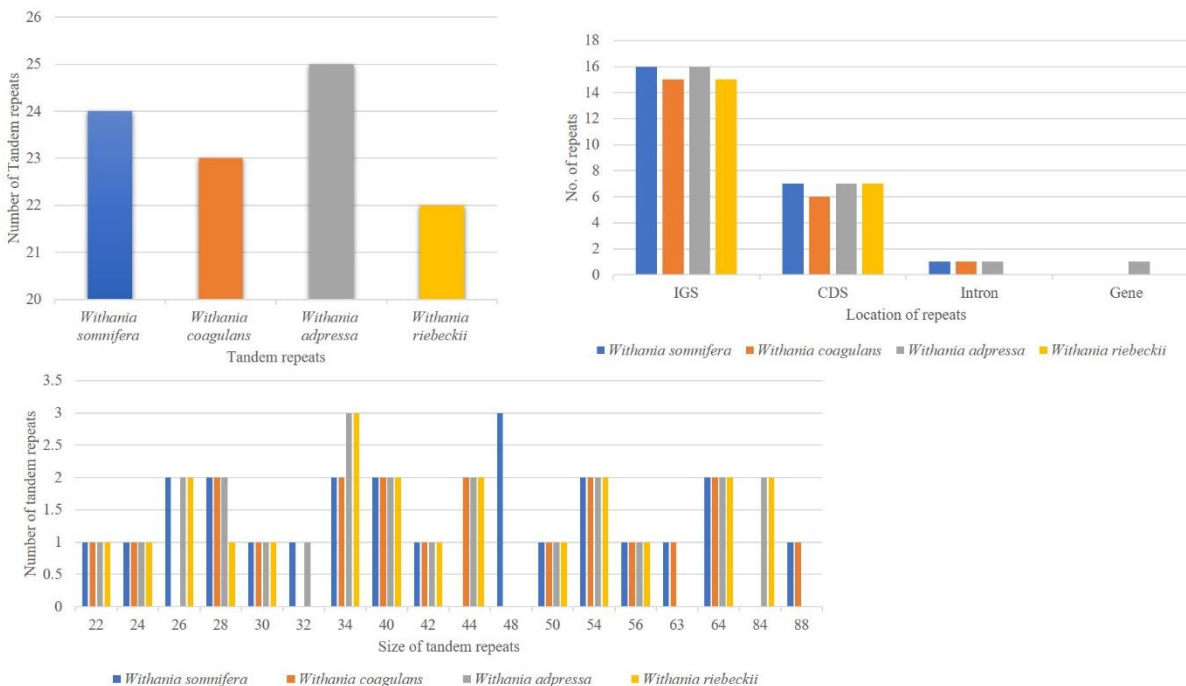


**Figure 7.** Comparison of tandem repeats among *Withania* (A) Number of tandem repeats in the chloroplast genomes (B) Location and number of tandem repeats (C) Tandem repeat number, size, distribution.

## Inverted Repeats

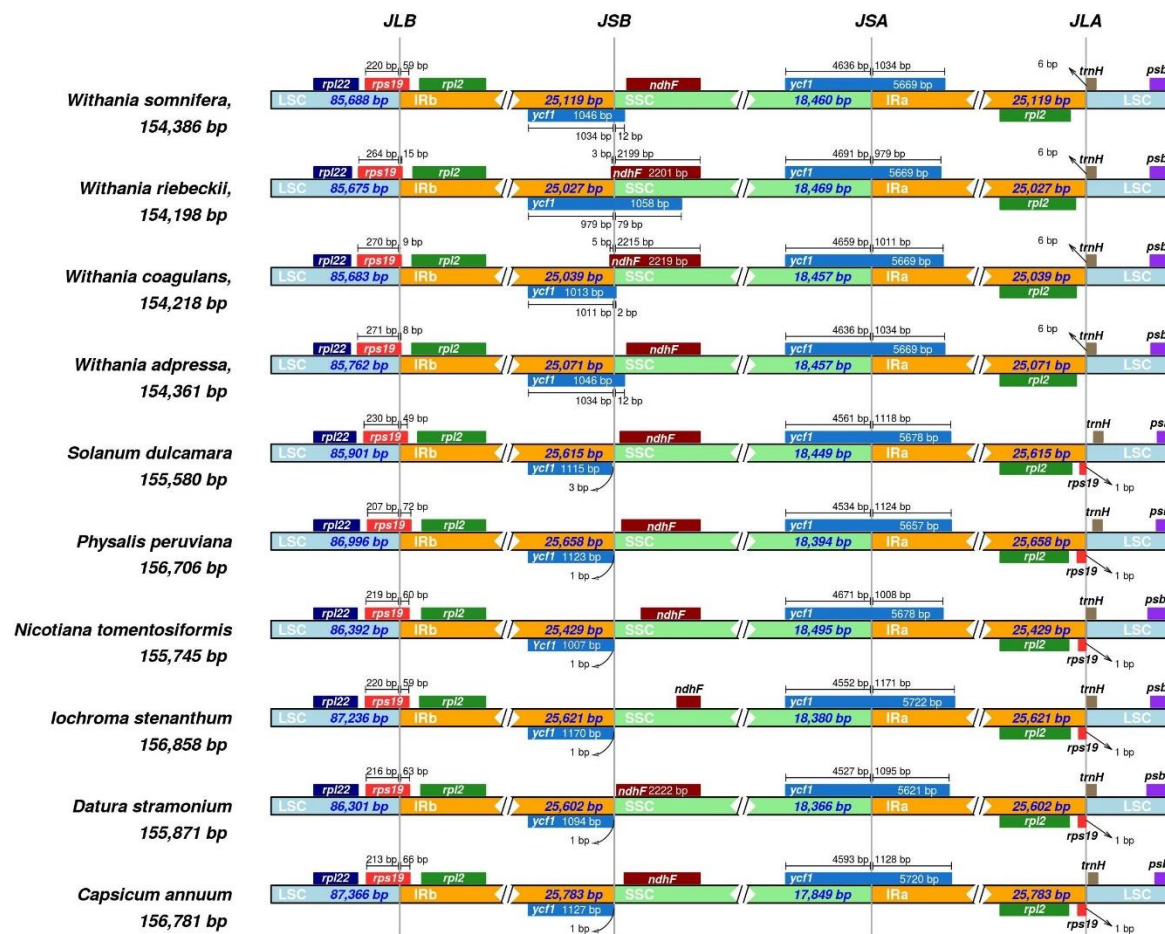


**Figure 8.** Comparison of the border positions of the large single-copy (LSC), small single-copy (SSC), and inverted repeat (IR) regions among the chloroplast genomes of four *Withania* species. The positive-strand transcribed genes are indicated under the line, while the genes that are transcribed by negative-strand are indicated above the line. Gene names are indicated in boxes, and their lengths of relative regions are shown above the boxes. The number of bp (base pairs) that are written with the genes revealed part of the genes that exist in or away from the region of the chloroplast, i.e. bp written with *ycf1* indicates that that sequence exists in that region of the plastid genome.

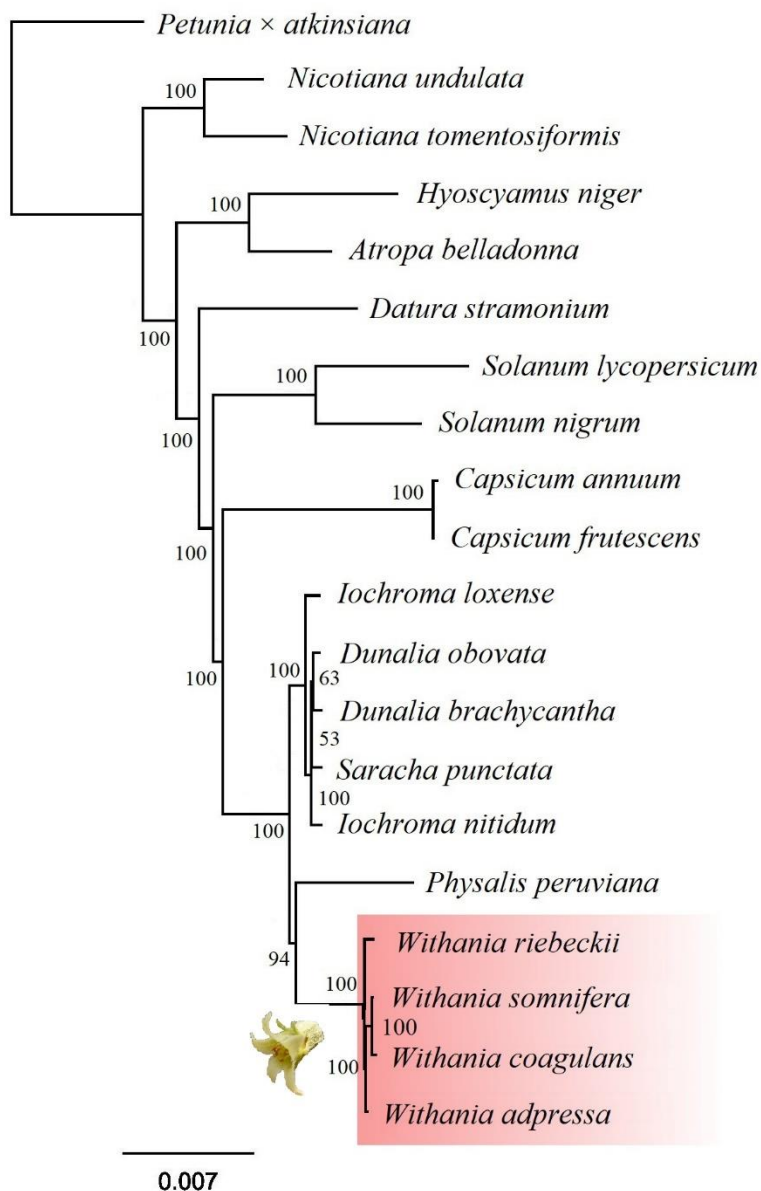


**Figure 9.** Maximum likelihood (ML) tree showing the position of *Withania* species. The tree was reconstructed based on 74 protein-coding plastid genes of 19 Solanaceae species. Numbers represent ultrafast bootstrap approximation scores.

**Table 1.** Comparison and general features of chloroplast genomes of *Withania somnifera*, *Withania adpressa*, *Withania coagulans*, *Withania riebeckii*.

Characteristics	<i>Withania somnifera</i>	<i>Withania coagulans</i>	<i>Withania adpressa</i>	<i>Withania riebeckii</i>	
Size (base pair; bp)	154,386	154,216	154,361	154,198	
LSC length (bp)	85,688	85,683	85,760	85,675	
SSC length (bp)	18,464	18,457	18,457	18,469	
IR length (bp)	25,117	25,038	25,071	25,027	
Number of genes	132	132	132	132	
Protein-coding genes	86	86	86	86	
tRNA genes	37	37	37	37	
rRNA genes	8	8	8	8	
Duplicate genes	18	18	18	18	
GC content	Total (%)	37.7%	37.7%	37.7%	37.7%
	LSC (%)	35.7%	35.7%	35.7%	35.7%
	SSC (%)	31.8%	31.8%	31.8%	31.8%
	IR (%)	43.2%	43.2%	43.2%	43.2%
	CDS (%)	38.2%	38.2%	38.2%	38.2%
	rRNA (%)	55.3%	55.3%	55.3%	55.3%
	tRNA (%)	53%	52.9%	53%	53%
All gene %	40%	39.8%	39.8%	39.8%	
Protein coding part (CDS) (%bp)	50.9%	51.0%	51.0%	51.0%	
All gene (%bp)	72.06%	72.11%	72.07%	72.13%	
Non-coding region (%bp)	27.94%	27.89%	27.93%	27.87%	

**Table 2.** Genes of chloroplast genomes of *Withania adpressa*, *Withania coagulans*, *Withania riebeckii*.

Category for gene	Group of gene	Name of gene				
Photosynthesis-related genes	Photosystem I	<i>psaA</i>	<i>psaB</i>	<i>psaC</i>	<i>psaI</i>	<i>psaJ</i>
	Photosystem II	<i>psbA</i>	<i>PsbB</i>	<i>psbC</i>	<i>psbD</i>	<i>psbE</i>
		<i>psbF</i>	<i>psbH</i>	<i>psbI</i>	<i>psbJ</i>	<i>psbK</i>
		<i>psbL</i>	<i>psbM</i>	<i>psbN</i>		
	Cytochrome b/f complex	<i>psbT</i>	<i>psbZ</i>	<i>petN</i>	<i>petA</i>	<i>petL</i>
		<i>petG</i>	<i>petD*</i>	<i>petB*</i>		
	ATP synthase	<i>atpI</i>	<i>atpH</i>	<i>atpA</i>	<i>atpF*</i>	<i>atpE</i>
		<i>atpB</i>				
	Assembly/stability of photosystem I	<i>ycf3**</i>	<i>ycf4</i>			
	NADPH dehydrogenase	<i>ndhB*,<sup>a</sup></i>	<i>ndhH</i>	<i>ndhA*</i>	<i>ndhI</i>	<i>ndhG</i>
<i>ndhJ</i>		<i>ndhE</i>	<i>ndhF</i>	<i>ndhC</i>	<i>ndhK</i>	
<i>ndhD</i>						
Rubisco	<i>rbcL</i>					
Transcription and translation related genes RNA genes	Transcription Small subunit of ribosome	<i>rpoA</i>	<i>rpoC2</i>	<i>rpoC1*</i>	<i>rpoB</i>	<i>rps16*</i>
		<i>rps7<sup>a</sup></i>	<i>rps15</i>	<i>rps19</i>	<i>rps3</i>	<i>rps8</i>
		<i>rps14</i>	<i>rps11</i>	<i>rps12<sup>a,*</sup></i>	<i>rps18</i>	<i>rps4</i>
		<i>rps2</i>				
	Large subunit of ribosome	<i>rpl2<sup>a,*</sup></i>	<i>rpl23<sup>a</sup></i>	<i>rpl32</i>	<i>rpl22</i>	<i>rpl14</i>
		<i>rpl33</i>	<i>rpl36</i>	<i>rpl20</i>	<i>rpl16*</i>	
	Ribosomal RNA	<i>rrn16<sup>a</sup></i>	<i>rrn4.5<sup>a</sup></i>	<i>rrn5<sup>a</sup></i>	<i>rrn23<sup>a</sup></i>	
	Transfer RNA	<i>trnV-GAC<sup>a</sup></i>	<i>trnI-CAU*</i>	<i>trnA-UGC<sup>a,*</sup></i>	<i>trnN-GUU<sup>a</sup></i>	<i>trnP-UGG</i>
		<i>trnW-CCA,</i>	<i>trnV-UAC*</i>	<i>trnL-UAA*</i>	<i>trnF-GAA</i>	<i>trnRACG<sup>a</sup></i>
		<i>trnT-UGU</i>	<i>trnG-UCC<sup>a,*</sup></i>	<i>trnT-GGU</i>	<i>trnR-UCU</i>	<i>trnE-UUC</i>
		<i>trnY-GUA</i>	<i>trnD-GUC</i>	<i>trnC-GCA</i>	<i>trnS-GCU</i>	<i>trnH-GUG</i>
		<i>trnK-UUU</i>	<i>trnQ-UUG</i>	<i>trnM-CAU</i>	<i>trnG-GCC</i>	<i>trnS-UUA</i>
		<i>trnS-GGA</i>	<i>trnF-GAA</i>	<i>trnM-CAU</i>	<i>trnL-CAA*</i>	
		<i>trnI-GAU*<sup>a</sup></i>	<i>trnL-UAG</i>			
	Other genes	RNA processing	<i>matK</i>			
		Carbon metabolism	<i>cemA</i>			
		Fatty acid synthesis	<i>accD</i>			

	Proteolysis	<i>clpP</i> **				
	Component of TIC complex	<i>ycf1</i> <sup>a</sup>				
	Hypothetical proteins	<i>ycf2</i> <sup>a</sup>	<i>Ycf15</i>			

\* Gene with one intron, \*\* Gene with two introns, <sup>a</sup> Gene with two copies, Same genes in all *Withania* species.

**Table 3.** Comparison of substitution in *Withania* species

Types	<i>Withania coagulans</i>	<i>Withania adpressa</i>	<i>Withania riebeckii</i>
A/G	4	20	26
C/T	13	15	26
A/C	3	11	17
C/G	2	3	4
G/T	1	14	25
A/T	5	4	12
Total	28	67	110
LSC	22	44	79
SSC	0	20	31
IR	6	3	8

*Withania somnifera* was used as reference for SNPs detection.

**Table 4.** Distribution of InDels in *Withania* chloroplast genome.

	<i>Withania coagulans</i>	InDel length (bp)	InDel average length
LSC	29	105	3.621
SSC	5	49	9.80
IR	8	87	10.87
	<i>Withania adpressa</i>	InDel length (bp)	InDel average length
LSC	30	146	4.867
SSC	6	11	1.833
IR	6	72	12.0
	<i>Withania riebeckii</i>	InDel length (bp)	InDel average length
LSC	34	163	4.794
SSC	6	103	17.16
IR	4	104	26.0

**Table 5.** Mutational hotspots among *Withania* species.

S. No	Region	Nucleotide Diversity	Total number of InDel sites	Number of sites
1	<i>rps16-trnQ-UUG</i>	2.5	31	1229
2	<i>rbcL-accD</i>	2.5	20	783
3	<i>clpP</i>	2.49333	8	1999
4	<i>trnL-UAA-trnF-GAA</i>	1.667	11	300
5	<i>ndhA</i>	2.08808	10	2254
6	<i>petN-psbM</i>	1.5	4	737
7	<i>trnT-psbD</i>	1.5	9	1176
8	<i>trnP-UGG-psaJ</i>	1.5	7	429
9	<i>trnI-ycf2</i>	1.5	8	88
10	<i>rpl32-trnL-UAG</i>	1.5	3	856
11	<i>rpl14-rpl16</i>	1.167	2	125
12	<i>trnK-UUU-rps16</i>	1	2	678
13	<i>rpoB-trnC-GCA</i>	1	11	1313
14	<i>ycf3</i>	1	2	1993
15	<i>petG-trnW-CCA</i>	1	2	131
16	<i>clpP-psbB</i>	1	2	445
17	<i>ycf15-trnV-GAC</i>	1.00509	12	498